catalysts

MDPI

Article

Quantitative Study of the Enhanced Content and Chemical Stability of Functional Groups in Mesoporous Silica by In-Situ Co-Condensation Synthesis

Hao Zha [1], Tongxiao Zhou [1], Fengli Gan [1], Bangda Wang [1,2,*], Zhongde Dai [1,2] and Xia Jiang [1,2]

[1] College of Architecture and Environment, Sichuan University, Chengdu 610065, China; 2019141470340@stu.scu.edu.cn (H.Z.); scuztx@163.com (T.Z.); 2021323050027@stu.scu.edu.cn (F.G.); zhongde.dai@scu.edu.cn (Z.D.); xjiang@scu.edu.cn (X.J.)

[2] National Engineering Research Center for Flue Gas Desulfurization, Chengdu 610065, China

* Correspondence: wang_bd@scu.edu.cn

Abstract: The chemical stability and content of organic functional groups significantly affect the application of materials in the field of adsorption. In this study, we quantitatively studied the effect of in-situ co-condensation and post grafting on the physico-chemical properties and sorption properties of modified mesoporous silica. The results showed that the grafting method changed the morphology of mesoporous silica while the in-situ method kept the spherical morphology well, and the amino groups were both successfully introduced into the materials. Besides, the amino content of the material prepared by in-situ method (ami-MSN) was 2.71 mmol/g, which was significantly higher than the 0.98 mmol/g of the grafting method (ami-g-MS). Moreover, the chemical stability of functional groups in ami-MSN was much better than ami-g-MS. Furthermore, ami-MSN showed better capability in removing toxic metals of Pb, Cd, Ni, and Cu, and the removal efficiency of Pb reached 98.80%. Besides, ami-MSN exhibited higher dynamic CO_2 adsorption of 0.78 mmol/g than ami-g-MS of 0.34 mmol/g. This study revealed the relationship between modification methods and the modification efficiency, functional groups stability, and sorption properties through quantitative comparative studies, which provided a reference for preparing modified mesoporous silica materials with high sorption properties.

Keywords: mesoporous silica; in-situ co-condensation; functionalization; quantitative study; sorbent; toxic metals; CO_2 capture

Citation: Zha, H.; Zhou, T.; Gan, F.; Wang, B.; Dai, Z.; Jiang, X. Quantitative Study of the Enhanced Content and Chemical Stability of Functional Groups in Mesoporous Silica by In-Situ Co-Condensation Synthesis. *Catalysts* **2022**, *12*, 620. https://doi.org/10.3390/catal12060620

Academic Editor: Lucjan Chmielarz

Received: 18 May 2022
Accepted: 3 June 2022
Published: 6 June 2022

1. Introduction

Mesoporous silica, due to its large specific surface area, abundant pore structure, excellent chemical stability, and good accessibility, has a wide range of applications in the field of adsorption and separation [1–4]. However, having a single mesoporous structure and being easily to agglomerate as a result of excess hydroxyl groups, mesoporous silica has its limitations in practical adsorption applications [5]. To improve its sorption properties, many studies were conducted to modify mesoporous silica by introducing functional groups such as sulfhydryl and amino groups onto the material surface [6–11]. The functionalization methods mainly include the traditional grafting method and in-situ co-condensation method (which has been developed in recent years).

Among these methods, the grafting method treats the prepared silica gel with an organosiloxane, and the corresponding functional groups are grafted to the surface of the silica through the action of the silicon hydroxyl group on the surface of the silica [12–14]. The advantage of grafting method is that we can control the structure, morphology, partical size, and pore size of modified mesoporous silica more easily [5]. The grafting method also has a little restriction to modified substances, and thus has become an important method in modification. However, the functional groups obtained by the grafting method tend to have

low structural stability and the functional groups are unevenly distributed in the pores and surfaces [15]. Hence, in-situ co-condensation synthesis has been more and more extensively used for functional modification of mesoporous silica in recent years [16]. Not only since it is simper with less synthetic procedures, but also under such synthesis condition, the organic functional groups are grafted into the inorganic network through chemical bonding, which means the formed functional groups has better chemical stability and vaster distribution both on the surface and in pore channels [17]. Until now, there have been many reports on the preparation of functionalized materials by those two methods [18,19]. However, in previous studies, the advantages in functional groups content and stability prepared by two methods were only qualitative and indirect studies, emphatically characterizing the property difference of materials before and after modification [20]. Meanwhile, since the sorption properties are closely related to functional groups and the stability of functional groups significantly affects the practical performance of materials, so it is important to pay attention to these aspects in modified materials. However, quantitative comparative studies of modification efficiency and functional groups stability between two methods were almost neglected. Moreover, the specific effects of different modification methods on sorption properties have not been quantified studied. Hence, it is essential to fill the gap of quantitative comparative studies about two methods on modification efficiency, functional groups stability and sorption properties, which is of great significance to guide subsequent product modification.

Herein, in this work, two kinds of modified mesoporous silica were successfully synthesized by grafting and in-situ co-condensation method. Furthermore, the modification efficiency and the functional groups stability of materials were contrastively studied. Moreover, the sorption properties of materials in the treatment of toxic metal-containing wastewater and the CO_2 capture capacity were compared. This work quantified the difference of two mesoporous silica modification methods, and provided a reference for the preparation of adsorption materials with good sorption properties in follow-up research.

2. Results and Discussions

2.1. Material Characterizations

The microstructures of ami-g-MS and ami-MSN were observed by SEM. As shown in Figure 1a, it could be found that ami-g-MS was amorphous and the structure was broken and loose, which was quite different from common unmodified mesoporous silica material of nanospheres [21]. Compared with ami-g-MS, ami-MSN (shown in Figure 1b) were consisted of uniform nanospheres. The spherical morphology indicated that the in-situ co-condensation could introduce amino functional groups mildly without damaging the original skeleton structure. The spherical structure could benefit the mass transfer performance [22], which may promote the sorption capacity of ami-MSN.

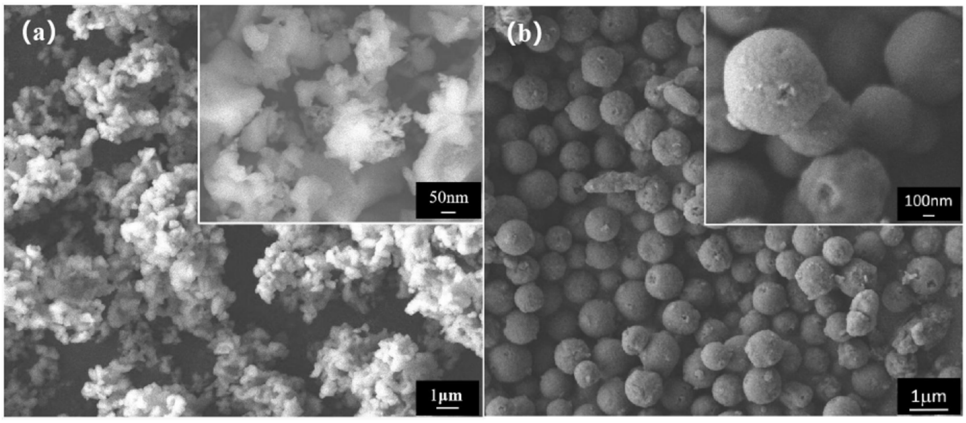

Figure 1. SEM images of (**a**) for ami-g-MS and (**b**) for ami-MSN.

The functional structures of ami-g-MS and ami-MSN were studied by FT-IR. As shown in Figure 2, the adsorption peak at 1082 cm^{-1} denotes the vibration of Si−O_{nb} and the peaks at 400–800 cm^{-1} denote the vibration of Si−O_{br} [23]. These absorption peaks suggest the framework structure of $SiO_2 \cdot xH_2O$ [24]. The absorption peak at 2927 cm^{-1} relates to the stretching vibration of $-CH_2-$ in organosiloxane [25]. The broad band of medium intensity at 3436 cm^{-1} indicates the presence of primary aliphatic amines [26,27], the adsorption band at 1636 cm^{-1} belongs to primary amines [28,29]. However, the adsorption peaks at 3436 cm^{-1} and 1636 cm^{-1} could also be attributed to the stretching and flexural vibration of −OH in Si−OH and adsorbed water [30,31]. Hence, the existence of nitrogenous functional groups was further confirmed by C, H, and N elemental analysis. The results suggested that amino groups were both well introduced and maintained in the ami-g-MS and ami-MSN framework.

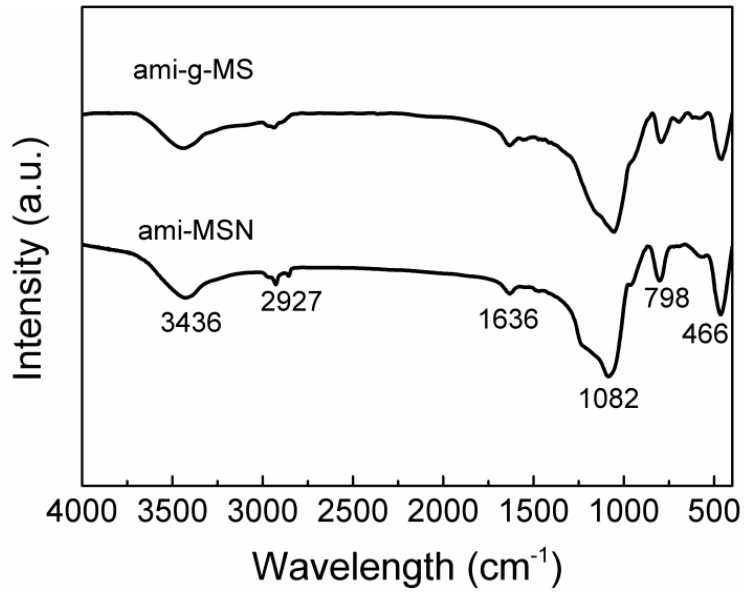

Figure 2. FT-IR spectra of ami-g-MS and ami-MSN.

Afterwards, the structures of materials were studied by ^{29}Si MAS-NMR. As shown in Figure 3, both materials showed four silicon species. Among them, the Q^3 and Q^4 species belonged to siloxane, where $Q^n = Si(OSi)_n(OH)_{4-n}$, n = 2–4. Both the T^3 and T^4 species belonged to organosiloxane, where $T^m = Rsi(Osi)_m(OH)_{3-m}$, m = 1–3. The presence of these chemical shifts indicated that the organosilicon and inorganic silicon formed ami-MSN via hydrolysis co-condensation, and the amino groups were distributed in the material framework via stable chemical bonding, which are consistent with the results of FT-IR. Meanwhile, ami-g-MS also exhibited a weak T^3 and T^4 chemical shifts, which may be due to the hydrolysis polycondensation of organosiloxane. Moreover, it was worth noting that the intensity of organosiloxane (T^m) NMR signals in ami-MSN was significantly stronger than that of ami-g-MS, which positively correlated with the content of organic functional groups [32]. This proved that the amino content in ami-MSN was higher than that of ami-g-MS.

Further, considering the amino groups were the only kind of functional groups in materials, the amino content could be measured by the content of the nitrogen element in the materials. The content of amino groups in the materials was determined by C, H, and N elemental analysis. As shown in Table 1, the nitrogen content of ami-MSN was 4.33%, and the content of the amino groups was calculated to be 2.71 mmol/g according to the structural formula of ami-MSN. While the nitrogen content of ami-g-MS was 1.58%, and the calculated amino groups density was only 0.98 mmol/g, which was significantly lower than that of ami-MSN. This may be attributed to that ami-g-MS was prepared by the direct grafting method, the grafting efficiency was not high and the amino groups

were more likely to distribute on the surface of the material. While the ami-MSN was obtained by in-situ organic-inorganic co-condensation method, the amino groups were stably distributed at the surface and also in the pores of ami-MSN framework. Moreover, for ami-g-MS, when demolding was carried out by calcination before grafting, the silanol groups (Si-OH) in oligomeric silica may lose a lot of groups, while ami-MSN extracted by extraction retained more Si-OH groups. Greater number of Si-OH groups and covalent bonds were formed with organic functional groups in inorganic framework, meaning that more amino functional groups could be loaded on ami-MSN.

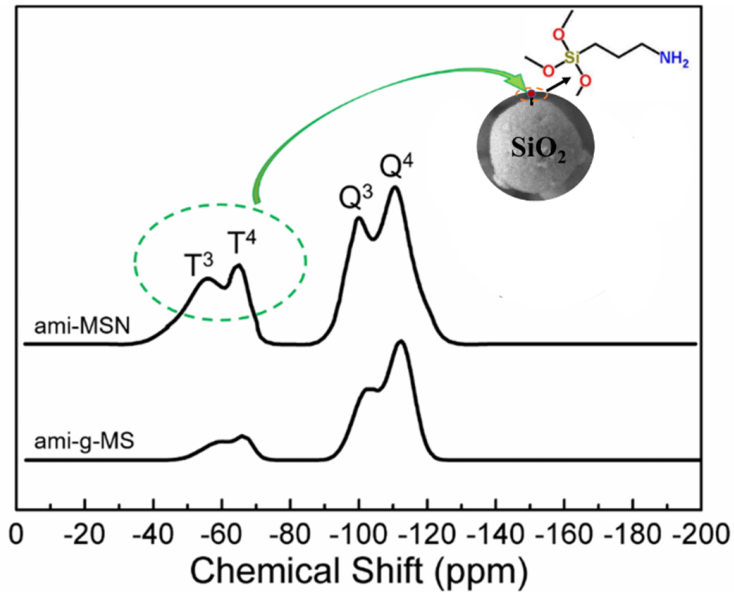

Figure 3. ^{29}Si MAS-NMR spectra of the amino-functionalized mesoporous silica. The spectra curves were treated using Guassian multi-peaks fitting.

Table 1. Elemental analysis of ami-g-MS and ami-MSN.

	C%	H%	N%	Amino Content
ami-MSN	12.99	3.69	4.33	2.71 mmol/g
ami-g-MS	10.17	2.84	1.58	0.98 mmol/g

The stability of the functional groups has significant influence on the performance of materials. Hence, the leakage of functional groups from material framework was studied. Since amino was the only functional group in materials, the stability of the amino groups can be analyzed by measuring the nitrogen leak rate of the materials in solution. Figure 4 showed the total nitrogen content of the materials contained in solution after shaking horizontally for a period of time. It can be seen that in the solution with ami-g-MS, the total nitrogen content increased significantly with time passing by. After 8 h of shaking, the total nitrogen content in the solution reached 40.2 mg/L, indicating a large number of amino groups leaked into solution. While for solution with ami-MSN, the total nitrogen content in the solution increased very slightly, which was only 0.38 mg/L after 8 h, indicating that just a few amino groups leaked into the solution. From above results, it could be concluded that the stability of the amino groups in ami-MSN was significantly better than that in ami-g-MS.

The above characterizations indicated that ami-MSN had better content and stability of functional groups. Hence, the specific surface area and mesoporous properties of ami-MSN were further measured through nitrogen adsorption-desorption isotherms. It can be seen from Figure 5 that the isotherms of ami-MSN belonged to the typical IV type isotherms according to IUPAC [33,34], which indicated a uniform porous distribution in the ami-MSN framework. The pore size distribution curve (smaller diagram in Figure 5) showed that its

main pore size was 3.2 nm, corroborating the presence of mesoporous structure. ami-MSN had a specific surface area of 465 m^2/g and pore volume of 0.38 cm^3/g. The large specific surface area and good pore structure indicated that ami-MSN had the potential of becoming an efficient adsorption material.

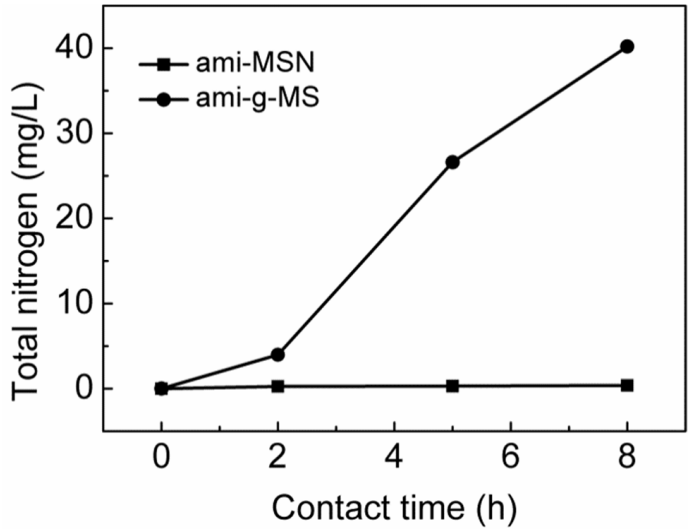

Figure 4. Total nitrogen content of solutions at different contact time for materials.

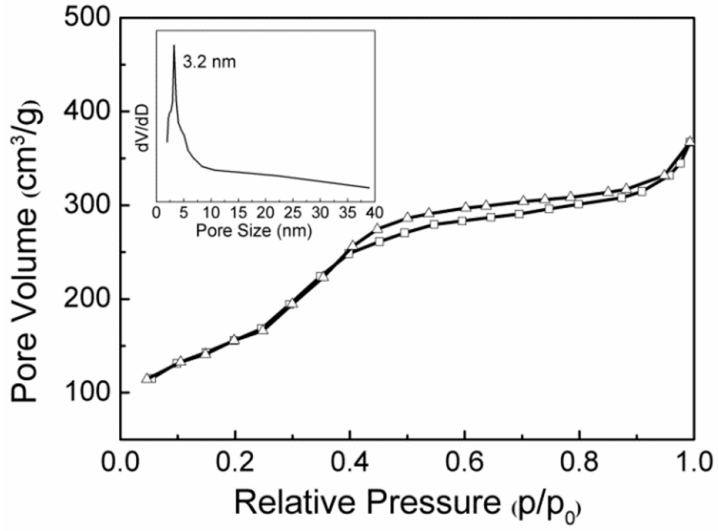

Figure 5. Nitrogen adsorption-desorption isotherms of ami-MSN, the smaller figure is the pore size distribution of ami-MSN.

2.2. Sorption Experiments

Furthermore, the sorption performance of ami-g-MS and ami-MSN were analyzed through two types of adsorption experiments. In the first place, the sorption property for toxic metals was studied. The wastewater from the battery plant was used, and the concentrations of primary metals in the original wastewater were shown in Table S1. A combination of CaO pretreatment and material adsorption purification treatment was applied to obtain better purification effect. Through pretreatment, trace amounts of toxic metals were remained. Then, the solution was filtered and subjected to treatment by prepared materials. As shown in Table 2, the removal efficiency of toxic metals such as Pb, Cd, Ni and Cu with ami-MSN was 98.80%, 95.80%, 96.20%, and 93.90%, respectively, which was much higher than that of ami-g-MS. This could be attributed to higher amino groups content in ami-MSN, which provided more amino chelating sites for metal ions [35]. The

ordered nanosphere morphology would also contribute since the morphology of adsorbent is an important factor affecting the adsorption performance of metal ions [2]. However, the sorption performance on other toxic metals such as Zn and Mn was poor both in ami-g-MS and ami-MSN, indicating the mount of amino groups had little impact on the removal efficiency of Zn and Mn. In summary, compared with ami-g-MS, ami-MSN prepared by in-situ co-condensation showed a much better removal effect on the purification of wastewater containing trace amount of specific toxic metals such as Pb, Cd, Ni, and Cu.

Table 2. Concentration of toxic metals (mg/L) before and after treatment.

		Pb	Cd	Ni	Cu	Zn	Mn
After pretreatment	Cp	5.60	4.10	12.20	8.90	5.60	1.70
MS	C_1	4.10	2.80	9.10	7.90	5.20	1.10
	R_1/%	26.80	31.70	25.40	11.20	21.20	35.30
ami-g-MS	C_2	0.86	1.62	2.42	1.24	5.00	1.20
	R_2/%	84.60	60.50	80.20	86.10	24.20	29.40
ami-MSN	C_3	0.07	0.17	0.46	0.54	5.10	1.30
	R_3/%	98.80	95.80	96.20	93.90	27.30	23.50

Note: C_p, C_1, C_2 and C_3 were the contents of each toxic metals (mg/L) in solution after pretreatment, MS adsorption, ami-g-MS adsorption and ami-MSN adsorption, respectively. R_1, R_2 and R_3 were the corresponding removal efficiencies of MS, ami-g-MS and ami-MSN, respectively ($R_x = 100 \times (C_x/C_p)$, x = 1, 2, 3).

Moreover, the CO_2 capture capacities of ami-g-MS and ami-MSN were studied. As shown in Figure 6, the mesoporous silica without amino introduced showed a CO_2 adsorption capacity of 0.06 mmol/g, showing knockdown CO_2 adsorption ability. This is due to the fact that the ultra-micropores with the size of 0.7–0.9 nm are most responsible for the high uptake of CO_2 (dynamic diameter of 0.33 nm) [36]. Mesopores with the pore size of 2–50 nm did not benefit from CO_2 adsorption, which accounted the most for pore size in MS [37]. After the introduction of amino groups, the CO_2 adsorption capacities of ami-g-MS and ami-MSN both had significant improvement. The adsorption capacity of ami-MSN reached 0.78 mmol/g, which was much higher than ami-g-MS of 0.34 mmol/g. It was clear that the quantity of amino groups was highly correlated with the adsorption capacity of CO_2 (Table 1 and Figure 6). These could be attributed to the strong interaction between basic amino groups and acidic CO_2 molecules. The above results indicated that compared with grafting, in-situ co-condensation method could be a potential effective modification method for preparing modified mesoporous silica-based CO_2 absorbent.

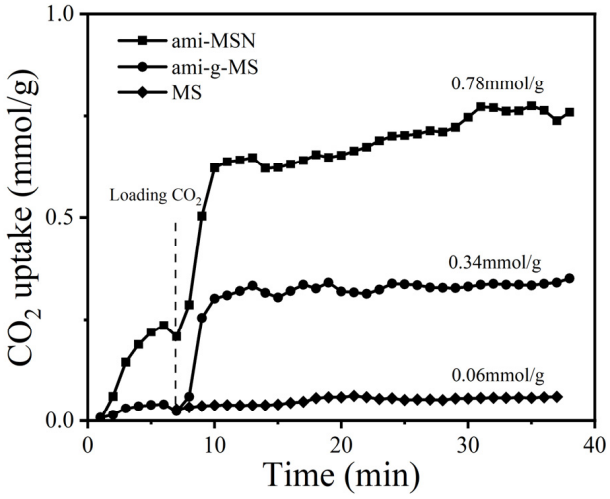

Figure 6. Dynamic CO_2 adsorption capacity of the materials.

3. Experimental

3.1. Chemicals

Sodium silicate, hydrochloric acid, absolute ethyl ethanol(ethanol for short), P123 (PEO-PPO-PEO block copolymer) and KH-550 (3-Aminopropyltriethoxysilane) were purchased from Sinopharm, China. The toxic metals contained wastewater kindly supplied by battery plant in Guangdong, China, which was generated from cleaning the equipment of production line and workshop ground.

3.2. Preparation of Materials

Synthesis of ami-g-MS: 160 mL of distilled water and 40 mL of HCl (36 wt%) were mixed and then 4.0 g of P123 was dissolved in it, the mixture was marked as A. Solution B was prepared by mixing KH-550, H_2O, ethanol with mass ratio of KH-550:H_2O:ethanol = 1:2:16, and the total weight was 95 g. Sodium silicate (10 g) were added in A and stirred for 12 h at 40 °C, then aging statically for 72 h at 100 °C. After that, the solid was separated by vacuum filtration. Further, the dried solid was calcinated at 600 °C for 4 h to remove surfactant, the solid obtained was marked as MS. Add 1.5 g MS to B and stirred for 24 h, then the solid was filtered and dried, marking it as ami-g-MS.

Synthesis of ami-MSN: The initial steps were the same as above, acquiring A. Afterward, sodium silicate (10 g) and KH-550 (5 g) were added in A and stirred for 12 h at 40 °C, then aging statically for 72 h at 100 °C. After that, the solid was separated by vacuum filtration and further put and stirred in 500 mL ethanol at 80 °C to remove the surfactant. Finally the solid was filtered and dried in a vacuum oven at 50 °C and marked as ami-MSN for follow-up studies.

3.3. Characterization

Concentration of toxic metals was analyzed by ICP-AES (ICPE-9000, Shimadzu Corporation, Kyoto, Japan). The microstructures of the materials were observed with a scanning electron microscope (SEM, Hitachi S-4800, Tokyo, Japan). FT-IR spectra was obtained through infrared spectrometer (Nicolet 6700, Thermo Fisher Scientific, Waltham, MA, USA). C, H, N elemental analysis was conducted on an elemental analyzer (Vario EL III, Elementar, Langenselbold, Germany). The 29Si-NMR tests were performed on NMR spectrometer (Bruker, Billerica, MA, USA). The stability of amino groups was analyzed by measuring the total nitrogen content in solution with a total nitrogen analyzer (multi N/C 2100, Analytik Jena AG, Jena, Germany). Nitrogen adsorption-desorption isotherms were measured at −196 °C with the Micromeritics ASAP 2020 system, the samples were pretreated using vacuum-pumping degassing at 200 °C for 12 h. The dynamic CO_2 adsorption capacity were analyzed by simultaneous thermal analyzer (STA 449 F3, Netzsch, Selb, Germany).

3.4. Determination of the Removal Efficiency of Template Agent

For removal efficiency of template agent: materials were calcined at 600 °C for 4 h. Weight changes were measured by TGA (Figure S1, Supplementary Materials).

3.5. Determination of the Stability of Functional Groups

0.3 g of material was added into 100 mL ultrapure water (18.2 MΩ·cm), and pH was adjusted to 4 by adding moderate trace metal grade HCl. The solution sample was put in shaker (300 r/min, 30 °C) for 8 h, sampling every 2 h for total nitrogen analysis.

3.6. Batch Sorption Experiments

For toxic metals wastewater treatment: the wastewater was pretreated by adding 0.5 g/L of CaO and stirred for 30 min (Table S1, Supplementary Materials), the suspension liquid was filtered. Then 0.1 g of sorbent was added into 50 mL of the filtered liquid (2 g/L dosage, the determination of dosage was shown in Experimental S3, Supplementary Materials), the liquid sample was put in shaker (300 r/min, 30 °C) for 4 h, filtered for

further analysis. For CO_2 capture: the samples were desorbed at 200 °C for 75 min in N2 environment and then cooled to 30 °C for CO_2 adsorption of 30 min.

4. Conclusions

In this study, two kinds of the amino-functionalized mesoporous silica (ami-g-MS and ami-MSN) were successfully prepared via grafting and in-situ co-condensation synthesis respectively. The characterization results showed that amino groups were both successfully introduced to the framework of ami-g-MS and ami-MSN. At the same time, in-situ co-condensation synthesis tremendously improved the content and stability of amino groups in modified materials compared with grafting. In addition, benefiting from higher content and better stability of amino groups, ami-MSN showed better removal ability of specific toxic metals (the removal efficiency of Pb and Ni reached 98.8% and 96.2%, respectively) and owned superiority in dynamic CO_2 adsorption capacity (0.78 mmol/g) compared with ami-g-MS (0.34 mol/g). This work filled the gap of quantitative comparative studies on modified mesoporous silica prepared by the grafting method and in-situ co-condensation method, and provided a reference for preparing modification materials with good sorption properties.

Supplementary Materials: The following supporting information can be downloaded at: https://www.mdpi.com/article/10.3390/catal12060620/s1. Figure S1: Thermal weight loss diagram of ethanol treated materials and calcine treated material; Table S1: Concentration of toxic metals (C_{0-p}, mg/L) before and after pretreatment; Figure S2: The removal efficiency of Pb (II) on ami-MSN and MS at different dosage; Figure S3: (a) Sorption kinetics of Pb (II) on ami-MSN. (b) Sorption isotherms of Pb (II) on ami-MSN; Figure S4: Zeta potential of ami-MSN as a function of pH. References [38–41] are cited in the supplementary materials.

Author Contributions: Conceptualization, B.W.; methodology, B.W. and T.Z.; validation, B.W. and Z.D.; data curation, H.Z.; formal analysis, H.Z.; investigation, F.G. and B.W.; resources, B.W. and X.J.; supervision, T.Z., F.G., B.W., Z.D. and X.J.; visualization, H.Z.; writing—original draft, H.Z. writing—review and editing, H.Z., T.Z. and B.W.; project administration, B.W. and X.J.; funding acquisition, B.W. All authors have read and agreed to the published version of the manuscript.

Funding: This research was funded by the National Natural Science Foundation of China (52100154) and Department of Science and Technology of Sichuan Province (2020YFH0109).

Data Availability Statement: The data presented in this study are available in Supplementary Materials.

Conflicts of Interest: The authors declare no conflict of interest.

References

1. Yuan, T.; Chen, Q.; Shen, X. Adsorption of cesium using mesoporous silica gel evenly doped by Prussian blue nanoparticles. *Chin. Chem. Lett.* **2020**, *31*, 2835–2838. [CrossRef]
2. Lee, J.Y.; Chen, C.H.; Cheng, S.; Li, H.Y. Adsorption of Pb(II) and Cu(II) metal ions on functionalized large-pore mesoporous silica. *Int. J. Environ. Sci. Technol.* **2016**, *13*, 65–76. [CrossRef]
3. Qiao, W.; Zhang, P.; Sun, L.; Ma, S.; Xu, W.; Xu, S.; Niu, Y. Adsorption performance and mechanism of Schiff base functionalized polyamidoamine dendrimer/silica for aqueous Mn(II) and Co(II). *Chin. Chem. Lett.* **2020**, *31*, 2742–2746. [CrossRef]
4. Zamani, C.; Illa, X.; Abdollahzadeh-Ghom, S.; Morante, J.R.; Rodriguez, A.R. Mesoporous Silica: A Suitable Adsorbent for Amines. *Nanoscale Res. Lett.* **2009**, *4*, 1303–1308. [CrossRef]
5. Sha, X.; Dai, Y.; Song, X.; Liu, S.; Zhang, S.; Li, J. The Opportunities and Challenges of Silica Nanomaterial for Atherosclerosis. *Int. J. Nanomed.* **2021**, *16*, 701–714. [CrossRef]
6. Li, J.; Miao, X.; Hao, Y.; Zhao, J.; Sun, X.; Wang, L. Synthesis, amino-functionalization of mesoporous silica and its adsorption of Cr(VI). *J. Colloid Interface Sci.* **2008**, *318*, 309–314. [CrossRef]
7. Chung, J.; Chun, J.; Lee, J.; Lee, S.H.; Lee, Y.J.; Hong, S.W. Sorption of Pb(II) and Cu(II) onto multi-amine grafted mesoporous silica embedded with nano-magnetite: Effects of steric factors. *J. Hazard. Mater.* **2012**, *239–240*, 183. [CrossRef]
8. Heidari, A.; Younesi, H.; Mehraban, Z. Removal of Ni(II), Cd(II), and Pb(II) from a ternary aqueous solution by amino functionalized mesoporous and nano mesoporous silica. *Chem. Eng. J.* **2009**, *153*, 70–79. [CrossRef]
9. Ghorbani, M.; Nowee, S.M.; Ramezanian, N.; Raji, F. A new nanostructured material amino functionalized mesoporous silica synthesized via co-condensation method for Pb(II) and Ni(II) ion sorption from aqueous solution. *Hydrometallurgy* **2016**, *161*, 117–126. [CrossRef]

10. Wang, S.; Wang, K.; Dai, C.; Shi, H.; Li, J. Adsorption of Pb 2+ on amino-functionalized core–shell magnetic mesoporous SBA-15 silica composite. *Chem. Eng. J.* **2015**, *262*, 897–903. [CrossRef]
11. Yokoi, T.; Kubota, Y.; Tatsumi, T. Amino-functionalized mesoporous silica as base catalyst and adsorbent. *Appl. Catal. A Gen.* **2012**, *421–422*, 14–37. [CrossRef]
12. Lei, X.; Zhang, A.; Zhang, F.; Liu, J. Preparation and characterization of a novel macroporous silica-bipyridine asymmetric multidentate functional adsorbent and its application for heavy metal palladium removal. *J. Hazard. Mater.* **2017**, *337*, 178–188.
13. Walcarius, A.; Etienne, M.; Lebeau, B. Rate of Access to the Binding Sites in Organically Modified Silicates. 2. Ordered Mesoporous Silicas Grafted with Amine or Thiol Groups. *Chem. Mater.* **2003**, *15*, 2161–2173. [CrossRef]
14. Shephard, D.S.; Zhou, W.; Maschmeyer, T.; Matters, J.M.; Roper, C.L.; Parsons, S.; Johnson, B.F.G.; Duer, M.J. Site-Directed Surface Derivatization of MCM-41: Use of High-Resolution Transmission Electron Microscopy and Molecular Recognition for Determining the Position of Functionality within Mesoporous Materials. *Angew. Chem. Int. Ed.* **2010**, *37*, 2719–2723. [CrossRef]
15. Zhang, A.; Wang, W.; Chai, Z.; Kuraoka, E. Modification of a novel macroporous silica-based crown ether impregnated polymeric composite with 1-dodecanol and its adsorption for some fission and non-fission products contained in high level liquid waste. *Eur. Polym. J.* **2008**, *44*, 3899–3907. [CrossRef]
16. Kang, H.J.H.; Ali, R.F.; Paul, M.T.Y.; Radford, M.J.; Andreu, I.; Lee, A.W.H.; Gates, B.D. Tunable functionalization of silica coated iron oxide nanoparticles achieved through a silanol-alcohol condensation reaction. *Chem. Commun.* **2019**, *55*, 10452–10455. [CrossRef]
17. Estevao, B.M.; Miletto, I.; Hioka, N.; Marchese, L.; Gianotti, E. Mesoporous Silica Nanoparticles Functionalized with Amino Groups for Biomedical Applications. *Chemistryopen* **2021**, *10*, 1251–1259. [CrossRef]
18. Rico, M.; Sepulveda, A.E.; Ruiz, S.; Serrano, E.; Berenguer, J.R.; Lalinde, E.; Garcia-Martinez, J. A stable luminescent hybrid mesoporous copper complex-silica. *Chem. Commun.* **2012**, *48*, 8883–8885. [CrossRef]
19. Tomer, V.K.; Malik, R.; Jangra, S.; Nehra, S.P.; Duhan, S. One pot direct synthesis of mesoporous SnO2/SBA-15 nanocomposite by the hydrothermal method. *Mater. Lett.* **2014**, *132*, 228–230. [CrossRef]
20. Walcarius, A.; Delacôte, C. Rate of Access to the Binding Sites in Organically Modified Silicates. 3. Effect of Structure and Density of Functional Groups in Mesoporous Solids Obtained by the Co-Condensation Route. *Chem. Mater.* **2003**, *15*, 4181–4192. [CrossRef]
21. Kazemzadeh, P.; Sayadi, K.; Toolabi, A.; Sayadi, J.; Zeraati, M.; Chauhan, N.P.S.; Sargazi, G. Structure-Property Relationship for Different Mesoporous Silica Nanoparticles and its Drug Delivery Applications: A Review. *Front. Chem.* **2022**, *10*, 823785. [CrossRef] [PubMed]
22. Lv, C.; Xu, L.; Chen, M.; Cui, Y.; Wen, X.; Wu, C.-e.; Yang, B.; Wang, F.; Miao, Z.; Hu, X.; et al. Constructing highly dispersed Ni based catalysts supported on fibrous silica nanosphere for low-temperature CO_2 methanation. *Fuel* **2020**, *278*, 118333. [CrossRef]
23. Rameli, N.; Jumbri, K.; Wahab, R.A.; Ramli, A.; Huyop, F. Synthesis and characterization of mesoporous silica nanoparticles using ionic liquids as a template. *J. Phys. Conf. Ser.* **2018**, *1123*, 012068. [CrossRef]
24. Walrafen, G.E.; Stone, J. Raman Spectral Characterization of Pure and Doped Fused Silica Optical Fibers. *Appl. Spectrosc.* **1975**, *29*, 337–344. [CrossRef]
25. Giraldo, L.; Moreno-Piraján, J.C. Study on the adsorption of heavy metal ions from aqueous solution on modified SBA-15. *Mater. Res.* **2013**, *16*, 745–754. [CrossRef]
26. Long, D.A. Infrared and Raman characteristic group frequencies. Tables and charts George Socrates John Wiley and Sons, Ltd., Chichester, Third Edition, 2001. Price £135. *J. Raman Spectrosc.* **2004**, *35*, 905. [CrossRef]
27. Saraswati, T.E.; Astuti, A.R.; Rismana, N. Quantitative analysis by UV-Vis absorption spectroscopy of amino groups attached to the surface of carbon-based nanoparticles. *IOP Conf. Ser. Mater. Sci. Eng.* **2018**, *333*, 012027. [CrossRef]
28. Takeda, M.; Iavazzo, R.E.S.; Garfinkel, D.; Scheinberg, I.H.; Edsall, J.T. Raman Spectra of Amino Acids and Related Compounds. IX. Ionization and Deuterium Substitution in Glycine, Alanine and β-Alanine1,2,3. *J. Am. Chem. Soc.* **1958**, *80*, 3813–3818. [CrossRef]
29. Yoncheva, K.; Popova, M.; Szegedi, A.; Mihaly, J.; Tzankov, B.; Lambov, N.; Konstantinov, S.; Tzankova, V.; Pessina, F.; Valoti, M. Functionalized mesoporous silica nanoparticles for oral delivery of budesonide. *J. Solid State Chem.* **2014**, *211*, 154–161. [CrossRef]
30. Ulfa, M.; Miftahul Jannah, A. Synthesis of Mesoporous Fe2o3/SBA-15 and its Application for Nickel (II) Ion Adsorption. *Orient. J. Chem.* **2018**, *34*, 420–427. [CrossRef]
31. Ulfa, M.; Prasetyoko, D. Infrared Spectroscopic and Scanning Electron Microscopy Study of Ibuprofen Loading onto the Molecular Sieve Mesoporous Silica SBA-15 Material. *Orient. J. Chem.* **2018**, *34*, 2631–2636. [CrossRef]
32. Margolese, D.; Melero, J.A.; Christiansen, S.C.; Chmelka, B.F.; Stucky, G.D. Direct Syntheses of Ordered SBA-15 Mesoporous Silica Containing Sulfonic Acid Groups. *Chem. Mater.* **2000**, *12*, 2448–2459. [CrossRef]
33. Ng, E.P.; Mintova, S. Nanoporous materials with enhanced hydrophilicity and high water sorption capacity. *Microporous Mesoporous Mater.* **2008**, *114*, 1–26. [CrossRef]
34. Xuan, W.; Zhu, C.; Liu, Y.; Cui, Y. Mesoporous metal-organic framework materials. *Chem. Soc. Rev.* **2012**, *41*, 1677–1695. [CrossRef] [PubMed]
35. Qu, W.; Feng, Y.; Xiong, T.; Li, Y.; Wahia, H.; Ma, H. Preparation of corn ACE inhibitory peptide-ferrous chelate by dual-frequency ultrasound and its structure and stability analyses. *Ultrason. Sonochem.* **2022**, *83*, 105937. [CrossRef] [PubMed]

36. Gan, F.; Wang, B.; Jin, Z.; Xie, L.; Dai, Z.; Zhou, T.; Jiang, X. From typical silicon-rich biomass to porous carbon-zeolite composite: A sustainable approach for efficient adsorption of CO_2. *Sci. Total Environ.* **2021**, *768*, 144529. [CrossRef] [PubMed]
37. Dong, S.; Zhu, M.; Dai, B. Synthesis of Alumina-Containing Hexagonal Mesoporous Silica and Its Application in the Adsorption of Gossypol. *Asian J. Chem.* **2013**, *25*, 525–528. [CrossRef]
38. Cho, H.-H.; Wepasnick, K.; Smith, B.A.; Bangash, F.K.; Fairbrother, D.H.; Ball, W.P. Sorption of AqueousZn II and Cd II by Multiwall Carbon Nanotubes: The Relative Roles of Oxygen-Containing Functional Groups and Graphenic Carbon. *Langmuir* **2010**, *26*, 967–981. [CrossRef]
39. Liu, Y. Some consideration on the Langmuir isotherm equation. *Colloids Surf. A-Physicochem. Eng. Asp.* **2006**, *274*, 34–36. [CrossRef]
40. Obrien, R.W.; Cannon, D.W.; Rowlands, W.N. Electroacoustic determination of particle-sizeand zeta-potential. *J. Colloid Interface Sci.* **1995**, *173*, 406–418. [CrossRef]
41. Barz, D.P.J.; Vogel, M.J.; Steen, P.H. Determination of the Zeta Potential of Porous Substrates byDroplet Deflection. I. The Influence of Ionic Strength and pH Value of an Aqueous Electrolyte in Contact with a Borosilicate Surface. *Langmuir* **2009**, *25*, 1842–1850. [CrossRef]